

# Effect of zinc substitution for calcium on the crystallisation of calcium fluoro-alumino-silicate glasses

Zhang, Siqi; Stamboulis, Artemis

DOI:

[10.1016/j.jnoncrysol.2015.10.025](https://doi.org/10.1016/j.jnoncrysol.2015.10.025)

License:

Creative Commons: Attribution-NonCommercial-NoDerivs (CC BY-NC-ND)

Document Version

Peer reviewed version

Citation for published version (Harvard):

Zhang, S & Stamboulis, A 2016, 'Effect of zinc substitution for calcium on the crystallisation of calcium fluoro-alumino-silicate glasses', *Journal of Non-Crystalline Solids*, vol. 432, no. B, pp. 300–306.

<https://doi.org/10.1016/j.jnoncrysol.2015.10.025>

[Link to publication on Research at Birmingham portal](#)

## Publisher Rights Statement:

After an embargo period this document is subject to a Creative Commons Attribution Non-Commercial No Derivatives license

Checked Jan 2016

## General rights

Unless a licence is specified above, all rights (including copyright and moral rights) in this document are retained by the authors and/or the copyright holders. The express permission of the copyright holder must be obtained for any use of this material other than for purposes permitted by law.

- Users may freely distribute the URL that is used to identify this publication.
- Users may download and/or print one copy of the publication from the University of Birmingham research portal for the purpose of private study or non-commercial research.
- User may use extracts from the document in line with the concept of 'fair dealing' under the Copyright, Designs and Patents Act 1988 (?)
- Users may not further distribute the material nor use it for the purposes of commercial gain.

Where a licence is displayed above, please note the terms and conditions of the licence govern your use of this document.

When citing, please reference the published version.

## Take down policy

While the University of Birmingham exercises care and attention in making items available there are rare occasions when an item has been uploaded in error or has been deemed to be commercially or otherwise sensitive.

If you believe that this is the case for this document, please contact [UBIRA@lists.bham.ac.uk](mailto:UBIRA@lists.bham.ac.uk) providing details and we will remove access to the work immediately and investigate.

Effect of zinc substitution for calcium on the crystallisation of calcium  
fluoro-alumino-silicate glasses

Siqi Zhang and Artemis Stamboulis\*

Biomaterials Group, School of Metallurgy and Materials, University of Birmingham,  
Edgbaston, Birmingham B15 2TT, UK

\*corresponding author: [a.stamboulis@bham.ac.uk](mailto:a.stamboulis@bham.ac.uk)

## ABSTRACT

A series of 25, 60, 75 and 100 mol% zinc substituted for calcium ionomer glasses of the composition  $4.5\text{SiO}_2\text{-}3\text{Al}_2\text{O}_3\text{-}1.5\text{P}_2\text{O}_5\text{-}3\text{CaO-}2\text{CaF}_2$  were produced following a well-established melt quench route. Similar glass compositions have been widely used in dentistry as the glass component in glass ionomer cements. The glasses crystallise to an apatite and mullite phase after appropriate heat treatments and are interesting materials for bone repair. Zinc is a bactericidal agent and has shown ability to stimulate osteogenesis. The new zinc containing glass compositions were characterized by Helium Pycnometer, DSC, TGA, SEM and EDX. The density of the zinc substituted glasses and glass-ceramics increased with increasing the zinc content as expected. The glass transition temperature decreased with zinc substitution, whereas the crystallization temperature increased with zinc substitution. Zinc substituted glasses lead to the formation of gahnite in expense of mullite. Fluorapatite formation was not favoured in high zinc content glass ceramics, whereas loss of fluorine in the form of  $\text{SiF}_4$  was suggested. SEM and EDX analysis showed significant changes in the morphology of glass ceramics with zinc substitution. The formation of gahnite during glass crystallization may open new application avenues for these materials in the field of semiconducting materials.

**Keywords:** fluoro-alumino-silicate glass, crystal phases, gahnite

## 1. Introduction

Calcium fluoro-alumino-silicate glasses are commonly used for the formation of polyalkenoate cements and have a range of applications especially in dentistry. Previous studies have shown that such glasses can crystallize to form fluorapatite [1-4]. Apatite and fluorapatite glass-ceramics have attracted a lot of interest due to apatite being an important mineral phase of tooth and bone. Recently, a strontium containing glass ceramic ( $4.5\text{SiO}_2\text{-}3\text{Al}_2\text{O}_3\text{-}1.5\text{P}_2\text{O}_5\text{-}3\text{SrO-}2\text{SrF}_2$ ) exhibiting a strontium fluorapatite phase was reported to be non-biodegradable and osteoconductive similar and comparable to a bioactive HA-bioglass composite that was used as control [5]. The above study established the osteointegration of the strontium containing glass ceramic during short term implantation in a rabbit model [6]. Although, a number of cation substitutions for calcium studies in the above glass composition have been reported and the cation size effect on the structure of the glass and glass ceramics has been investigated [5], the effect of Zn addition on the apatite-forming ability of this glass has not been reported.

Two zinc glass compositions have attracted research attention in the literature;  $\text{CaO-ZnO-SiO}_2$  and  $\text{Al}_2\text{O}_3\text{-ZnO-SiO}_2$  [7-9]. In the  $\text{CaO-ZnO-SiO}_2$  ternary system, zinc oxide acts as both a network modifier and an intermediate oxide like alumina as reported by R. Hill et al. [7]. In addition, the release of zinc enhances bone formation and mineralization by directly activating the aminoacyl-tRNA synthetase in osteoblastic cells as well as stimulating cellular protein synthesis [8]. Moreover, zinc is important for the function of the immune system and has been recognized as an

antibacterial agent [9, 10]. Due to the above mentioned advantages, zinc silicate glasses may have a great potential as cement formers and as glass ceramics in hard tissue replacement. However, reports suggest that the zinc glass based cements have inferior mechanical properties compared to the corresponding aluminosilicate glass based cements for use in clinical dentistry [11-13]. Recently, zinc was incorporated into a Ca-Si system, forming a material referred as hardystonite ( $\text{Ca}_2\text{ZnSi}_2\text{O}_7$ ), which possesses improved mechanical properties with increased bending strength and fracture toughness as compared to hydroxyapatite (HAP) [14]. Furthermore, reports on zinc oxide addition in bioactive glasses and phosphor-silicate glasses have shown that zinc addition results in a decrease in the solubility of glasses as well as cytotoxic effects at levels of zinc ion release of higher than 2 ppm [15, 16]. Due to the properties of glass and glass-ceramics being determined critically by their composition (network modifiers and their atomic environment), the crystallisation process and the microstructure, both the design and characterisation of these glasses play a very important role in the development of new medical glasses.

In the present study, addition of zinc oxide to the following ionomer glass composition  $4.5\text{SiO}_2\text{-}3\text{Al}_2\text{O}_3\text{-}1.5\text{P}_2\text{O}_5\text{-(}3\text{-x)}\text{CaO-(}2\text{-y)}\text{CaF}_2\text{-xZnO-yZnF}_2$  is expected to have an effect on the structure of the glass as well as the formed glass-ceramics. It is also expected that the produced glass ceramics might have stimulatory effects on bone formation. More importantly, if Zn would act as an intermediate oxide, this will allow the design of new aluminium free glass compositions for bioceramic applications as well as dental and bone cements.

The purpose of the present work was to study the influence of zinc substitution on the crystallisation and specifically the apatite forming ability of fluorine containing calcium-alumino-silicate glasses. All the substituted glasses are based on the composition of  $4.5\text{SiO}_2\text{-}3\text{Al}_2\text{O}_3\text{-}1.5\text{P}_2\text{O}_5\text{-}3\text{CaO-}2\text{CaF}_2$ , which can crystallise to fluorapatite (FAP) and mullite on appropriate heat treatments. The samples were all characterised by DSC, TGA, XRD, SEM and EDX in order to observe the effect of zinc substitution on the crystallisation of glasses.

## 2. Materials and Methods

### 2.1. Materials preparation

The molar composition of the fluorine containing alumino-silicate glasses is shown in Table 1. The glass components silicate dioxide ( $\text{SiO}_2$ ), aluminium oxide ( $\text{Al}_2\text{O}_3$ ), phosphorus pentoxide ( $\text{P}_2\text{O}_5$ ), calcium fluoride ( $\text{CaF}_2$ ), zinc oxide ( $\text{ZnO}$ ), zinc fluoride ( $\text{ZnF}_2$ ) and calcium carbonate ( $\text{CaCO}_3$ ), supplied by Sigma Aldrich, were weighed out to give approximately 100 g of glass for each composition.

**Table 1:** Molar composition of Zn substituted alumino-silicate glasses

| Glass code    | $\text{SiO}_2$ | $\text{Al}_2\text{O}_3$ | $\text{P}_2\text{O}_5$ | $\text{CaO}$ | $\text{CaF}_2$ | $\text{ZnO}$ | $\text{ZnF}_2$ |
|---------------|----------------|-------------------------|------------------------|--------------|----------------|--------------|----------------|
| <b>0%Zn</b>   | 4.5            | 3                       | 1.5                    | 3            | 2              | 0            | 0              |
| <b>25%Zn</b>  | 4.5            | 3                       | 1.5                    | 1.75         | 2              | 1.25         | 0              |
| <b>60%Zn</b>  | 4.5            | 3                       | 1.5                    | 0            | 2              | 3            | 0              |
| <b>75%Zn</b>  | 4.5            | 3                       | 1.5                    | 0            | 1.25           | 3            | 0.75           |
| <b>100%Zn</b> | 4.5            | 3                       | 1.5                    | 0            | 0              | 3            | 2              |

The oxide powders were well mixed in a plastic container and transferred to a platinum rhodium (Pt, 5% Rh) crucible. The crucible was then placed in an electric furnace (EHF 17/3, Lenton, UK) for a period of 1.5 hours at a temperature of 1450°C. The glass melt was then quenched into deionized water to prevent phase separation and crystallisation. The frit glasses were milled followed by sieving. Fine (<45µm) and coarse glass particles (45µm-100µm) were obtained for further analysis. X-ray diffraction showed that all glasses were amorphous with the exceptions of 75%Zn, that was possible to quench but was partly crystallised and 100%Zn that was crystallised in the crucible and was not possible to quench. It is worth mentioning, that the 75%Zn glass was still transparent. As this glass was partly crystallised it could not be directly compared to the rest of the amorphous glasses but it was included to the results as an example of the effect of high zinc substitution.

## **2.2 Characterisation of glasses and glass ceramics**

Differential scanning calorimetry was used in order to examine the thermal transitions of the glass compositions in the temperature range from 300 to 1300°C. The instrument used was a NETZSCH 404C DSC with pairs of matched platinum-rhodium crucibles. All the measurements were performed using 20 mg of glass samples in dry argon at a heating rate of 10°C/min. For the TGA measurements, the instrument used was a NETZSCH Thermal Analysis STA 449C with pairs of matched platinum-rhodium crucibles. All the measurements were performed with 20 mg of glass samples in dry argon at a heating rate of 10°C/min.

The density of glasses and glass ceramics was measured by a helium pycnometer

(AccuPyc II 1340 Series). The standard deviation of all measurements was less than 0.0009 g/cm<sup>3</sup>. The samples had a particle size of <45µm and the mass of the samples was approximately 1gr. In order to calculate the density of glasses and glass ceramics, the average of ten consecutive measurements was taken.

The oxygen density (OD) was calculated by using the following equation:

$$OD = D \times \frac{\text{no of moles of oxygens in the glass}}{\text{molecular weight of glass}} \quad (\text{Equation 1})$$

where D is the density of the glass measured by helium pycnometer.

X-ray powder diffraction was used in order to identify the crystal phases present and study the effect of cation substitution on the crystallisation of glasses. All glass samples were heat treated in a furnace at 1100°C for 1 hour. X-ray diffraction was then performed on the heat treated samples using a continuous scan between  $2\theta = 10^\circ$  and  $60^\circ$ , with a step size of  $2\theta = 0.0200^\circ$ . A Philips analytical X-Pert XRD was used with Cu KA at 40 kV and 40 mA.

An XL 30 SEM&EDX FEG electron microscope was used in order to investigate the morphology of the glass ceramics operated at 20 kV. Prior to characterisation all glass ceramics were etched with HF (10%). All the glass ceramic samples were coated with carbon using an SB250 coating machine. The standard deviation for EDX results was less than 0.15wt%.

### **3. Results**

#### **3.1 Density study of Zn Substituted Glasses and Glass Ceramics**

The measured density and oxygen density for zinc containing alumino-silicate glasses are shown in Figures 1 and 2. It is indicated, that the density increased proportionally



with zinc substitution with the lowest density for 0%Zn and the highest density for 60%Zn. In the case of 75%Zn, the density measured 3.03 g/cm<sup>3</sup> but cannot be compared directly to the rest of the glasses as this one was partly crystallised. Similarly, the oxygen density increased with increasing zinc substitution as shown in Figure 2.

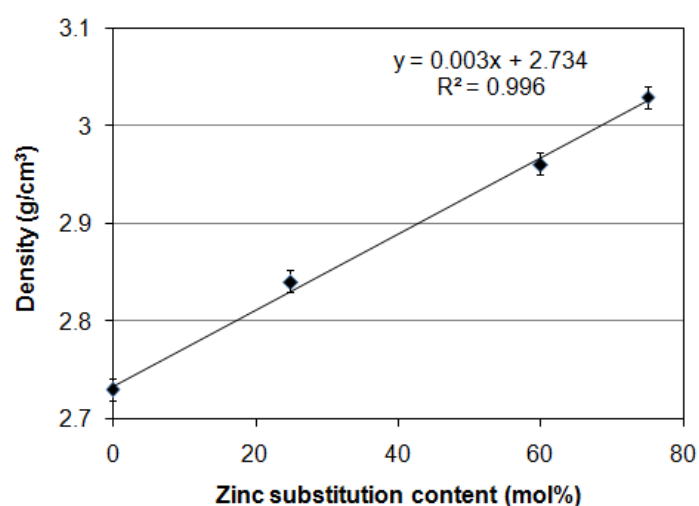


**Figure 1:** Density of zinc containing glasses.

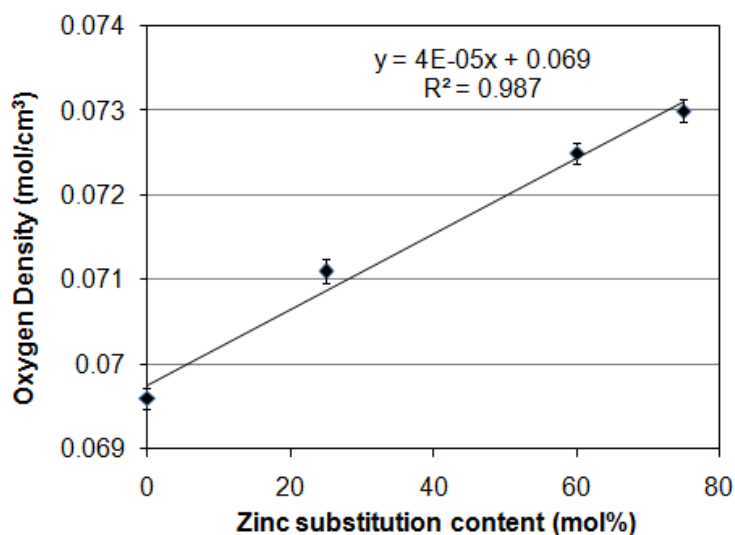


**Figure 2:** Oxygen density of zinc containing glasses.

In the case of glass ceramics, the density was increased with zinc substitution from

2.88 g/cm<sup>3</sup> for 0%Zn to 3.17 g/cm<sup>3</sup> for 75%Zn (Figure 3). It is clear, that there is a linear relationship between the density and the zinc molar content.

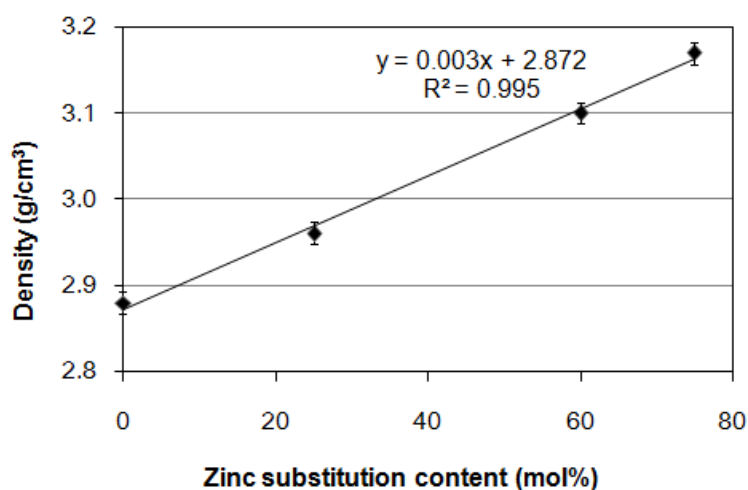


**Figure 3:** Density of zinc containing glass-ceramics.

### 3.2 DSC and TGA thermal analysis

Tables 2 and 3 present the glass transition, the crystallization and the crystal dissolution temperatures of both fine (<45μm) and coarse glass powders (>45 and <100μm). From Table 2, it is clear that the glass transition temperature of all fine glass powders decreased with zinc substitution. The first crystallisation temperature increased with substitution with the exception of the 75%Zn substitution, where a small decrease was observed compared to the 60%Zn substitution. As mentioned above 75%Zn glass was partly crystallised and cannot be directly compared to the amorphous glasses. It is interesting to note, that the second crystallisation temperature was not significantly affected by the substitution, whereas the crystal dissolution temperature exhibited a slight increase with zinc substitution.

**Table 2:** DSC analysis data for all Zn containing fine glass powders measured at a heating rate of 10°C /min.

| <b>Glass<br/>(fine particle<br/>size)</b> | <b>Zn content<br/>(molar %)</b> | <b>T<sub>g</sub>(°C )</b> | <b>T<sub>p1</sub>(°C )</b> | <b>T<sub>p2</sub>(°C )</b> | <b>Crystal<br/>dissolution<br/>temperature<br/>(°C)</b> |
|---|---------------------------------|---------------------------|----------------------------|----------------------------|---|
| <b>0%Zn</b>                               | 0                               | 655                       | 751                        | 934                        | ----  |
| <b>25%Zn</b>                              | 25                              | 625                       | 842                        | 947                        | 1161  |
| <b>60%Zn</b>                              | 60                              | 616                       | 943                        | ----                       | 1160, 1185  |
| <b>75%Zn</b>                              | 75                              | 595                       | 876                        | ----                       | 1244  |

**Table 3:** DSC analysis data for all Zn containing coarse glass powders obtained at a heating rate of 10°C /min.

| <b>Glass<br/>(coarse<br/>particle size)</b> | <b>Zn content<br/>(molar %)</b> | <b>T<sub>g</sub>(°C )</b> | <b>T<sub>p1</sub>(°C )</b> | <b>T<sub>p2</sub>(°C )</b> | <b>Crystal<br/>dissolution<br/>temperature<br/>(°C)</b> |
|---|---------------------------------|---------------------------|----------------------------|----------------------------|---|
| <b>0%Zn</b>                                 | 0                               | 667                       | 793                        | 1008                       | ---- [98]   |
| <b>25%Zn</b>                                | 25                              | 627                       | 933                        | 1032                       | 1173  |
| <b>60%Zn</b>                                | 60                              | 613                       | ----                       | ----                       | 1188  |
| <b>75%Zn</b>                                | 75                              | 616                       | ----                       | ----                       | 1255  |

From Table 3 on the other hand, it can be observed that the glass transition temperature of the coarse glass powders did not change significantly with substitution, whereas no crystallisation temperatures were observed for 60%Zn glass. A crystallisation temperature was also not observed for the partly crystallised 75%Zn glass. Crystal dissolution temperatures observed in the DSC graphs are shown in Figures 4, 5 (a) and 6 (a) as an endothermic transition.

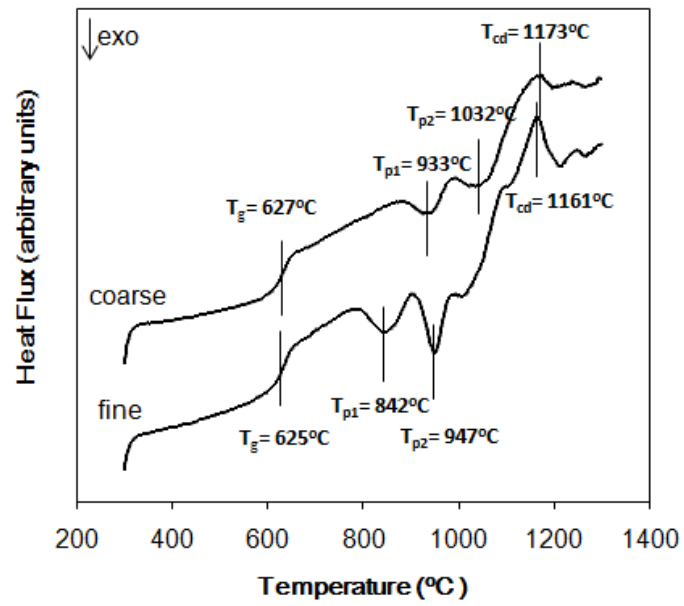


**Figure 4:** DSC traces of 25%Zn glass having different particle size (coarse and fine particle size) obtained at a heating rate of  $10^\circ\text{C}/\text{min}$ .

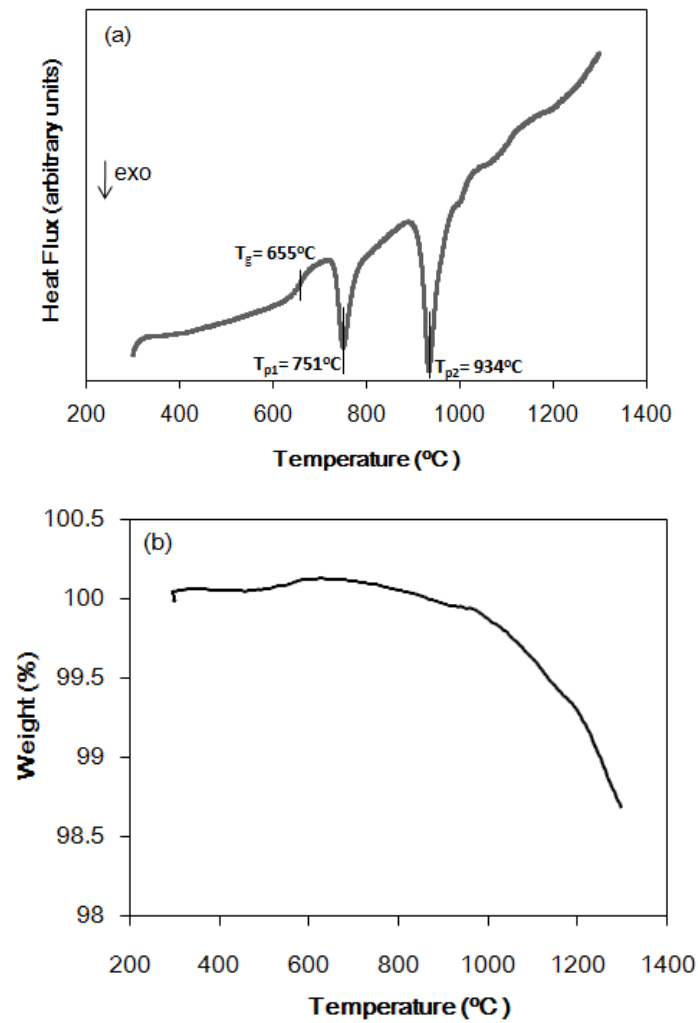


**Figure 5:** (a) DSC trace of 0%Zn glass (fine particle size) obtained at a heating rate of

10°C/min. (b) Thermogravimetric analysis of 0%Zn glass (fine particle size).

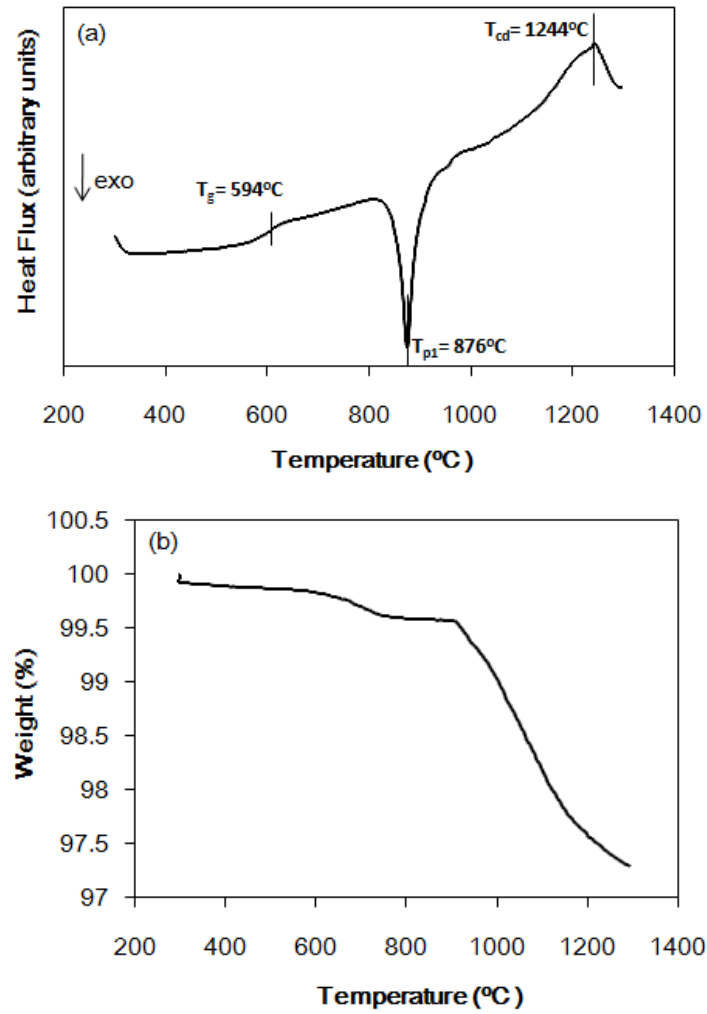


**Figure 6:** (a) DSC trace of 75%Zn glass (fine particle size) obtained at a heating rate of 10°C/min. (b) Thermogravimetric analysis of 75%Zn glass (fine particle size).

Since crystal dissolution temperatures were observed, one may think that crystallisation occurred very slowly. For this reason, isothermal measurements were conducted at 1000°C. The isothermal DSC graph for the 60%Zn coarse particle size glass is shown in Figure 7. The transition temperature did not change significantly and the crystallisation temperature was observed at 1000°C.

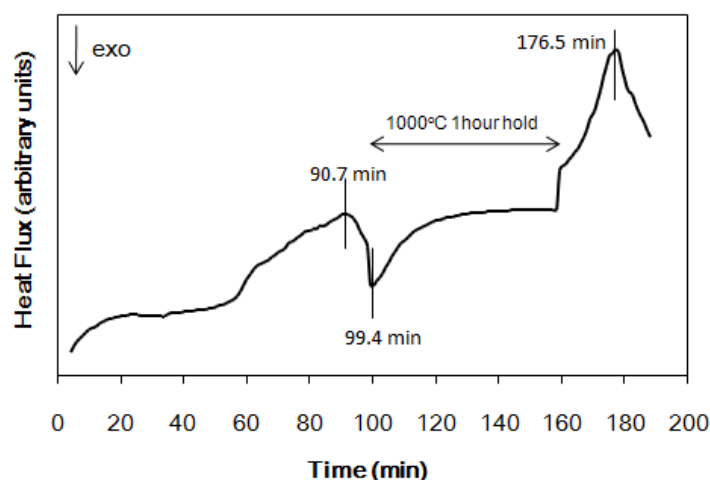


**Figure 7:** Isothermal DSC curve of 60%Zn (coarse particle size). One hour hold at 1000°C.

All fine particle size glasses exhibited one glass transition temperature, one or two crystallisation peak temperatures (Table 2) and another endothermic transition during which a small weight loss was observed in the TGA analysis shown in Figure 5(b) and 6 (b). The weight loss in glasses occurred in two stages: The temperature at which the first weight loss was recorded was 750 to 662°C, whereas the temperature at which the second weight loss (total 0.2%) was observed was around 1000°C. Above this temperature, the weight loss that was observed for all glasses was 1.25% with the exception of 75%Zn of which the weight loss increased to 2.3%. Generally, only a small weight loss was observed for all glasses with the partly crystallised 75%Zn substituted glass to have the highest.

### 3.3 XRD study of zinc substituted glasses and glass-ceramics

Table 4 presents the crystal phases formed after the crystallisation of glasses. Figure 8 (a) and (b) show the X-ray diffractograms of zinc substituted glasses and glass-ceramics. The 0%Zn glass was crystallised mainly to Ca fluorapatite

[Ca<sub>5</sub>(PO<sub>4</sub>)<sub>3</sub>F] and mullite (Al<sub>6</sub>Si<sub>2</sub>O<sub>13</sub>). Aluminium phosphate (AlPO<sub>4</sub>) was present as minor phase only.

**Table 4:** Main Crystal phases in zinc substituted glass-ceramics.

| Glass        | Crystal phases                                    |   |                   |                                  |   |
|--------------|---|---|-------------------|----------------------------------|---|
| <b>0%Zn</b>  | Ca <sub>5</sub> (PO <sub>4</sub> ) <sub>3</sub> F | Al <sub>6</sub> Si <sub>2</sub> O <sub>13</sub> | AlPO <sub>4</sub> | X                                | X   |
| <b>25%Zn</b> | Ca <sub>5</sub> (PO <sub>4</sub> ) <sub>3</sub> F | Al <sub>6</sub> Si <sub>2</sub> O <sub>13</sub> | AlPO <sub>4</sub> | ZnAl <sub>2</sub> O <sub>4</sub> | X   |
| <b>60%Zn</b> | Ca <sub>5</sub> (PO <sub>4</sub> ) <sub>3</sub> F | SiO <sub>2</sub><br>(cristobalite)              | AlPO <sub>4</sub> | ZnAl <sub>2</sub> O <sub>4</sub> | CaZn <sub>2</sub> (PO <sub>4</sub> ) <sub>2</sub> |
| <b>75%Zn</b> | Ca <sub>5</sub> (PO <sub>4</sub> ) <sub>3</sub> F | SiO <sub>2</sub><br>(cristobalite)              | AlPO <sub>4</sub> | ZnAl <sub>2</sub> O <sub>4</sub> | CaZn <sub>2</sub> (PO <sub>4</sub> ) <sub>2</sub> |

Figure 8 (b) represents the diffractogram of the 25%Zn substituted crystallised glass. Gahnite (ZnAl<sub>2</sub>O<sub>4</sub>) and fluorapatite were the major phases, whereas AlPO<sub>4</sub> was again a minor phase. The diffractogram of 60%Zn crystallised glass shown in Figure 8 (b) suggested that gahnite (ZnAl<sub>2</sub>O<sub>4</sub>) was the major phase. Calcium zinc phosphate [CaZn<sub>2</sub>(PO<sub>4</sub>)<sub>2</sub>], fluorapatite and cristobalite (SiO<sub>2</sub>) were also present, whereas AlPO<sub>4</sub> was again a minor phase. Figure 8 (b) shows also the X-ray diffractogram of 75%Zn crystallised glass. Similarly to 60%Zn glass ceramic, it is suggested that the glass was crystallised to gahnite, calcium zinc phosphate and a small amount of fluorapatite and cristobalite, whereas AlPO<sub>4</sub> was again present as a minor phase.

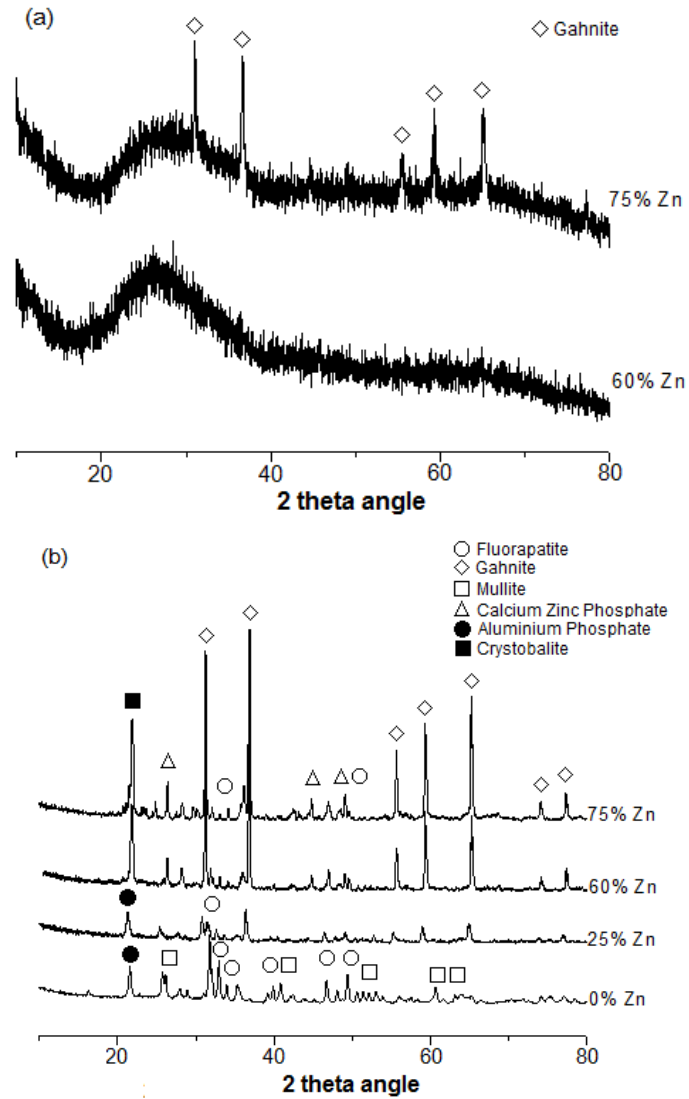


**Figure 8:** (a) X-ray diffractograms of 60% and 75% zinc substituted glasses, (b) X-ray diffractograms of glass-ceramics with different Zn substitutions.

### 3.3 SEM and EDX studies of Zn substituted glass-ceramics

Figure 9 shows an SEM micrograph and EDX analysis for the calcium base glass ceramic. A needle like morphology was observed for the glass ceramic corresponding to fluorapatite crystal phase interlocking with the mullite phase.



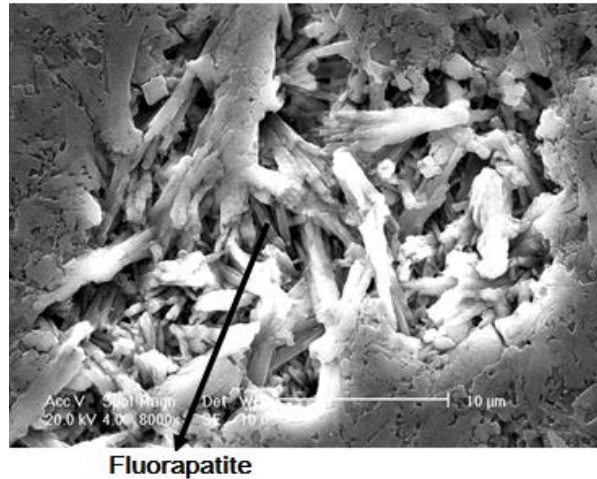


**Figure 9:** SEM and EDX analysis of 0%Zn glass-ceramic.

Figures 10-11 show the microstructure and morphology of different zinc substituted glass-ceramics. Figure 10 represents the SEM and EDX analysis for 25%Zn glass ceramic. The etched surface of the glass ceramic was very similar to the etched surfaces observed in previous work where needle-like fluorapatite was present [5]. EDX and XRD analysis showed that gahnite was a new phase formed when Zn was substituted for Ca. Figure 11 shows the SEM and EDX analysis of 60% and 75%Zn glass ceramics. It is clear that fluorapatite was still present as a needle-like phase, whereas gahnite exhibited a polygonal crystal morphology [12].

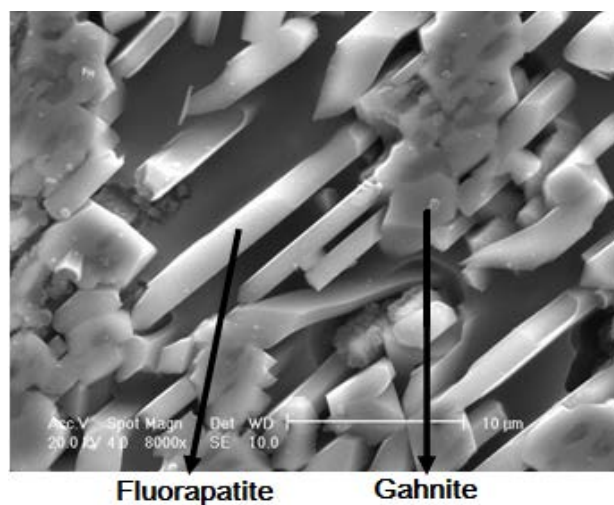


**Figure 10:** SEM and EDX analysis of 25%Zn glass-ceramic.

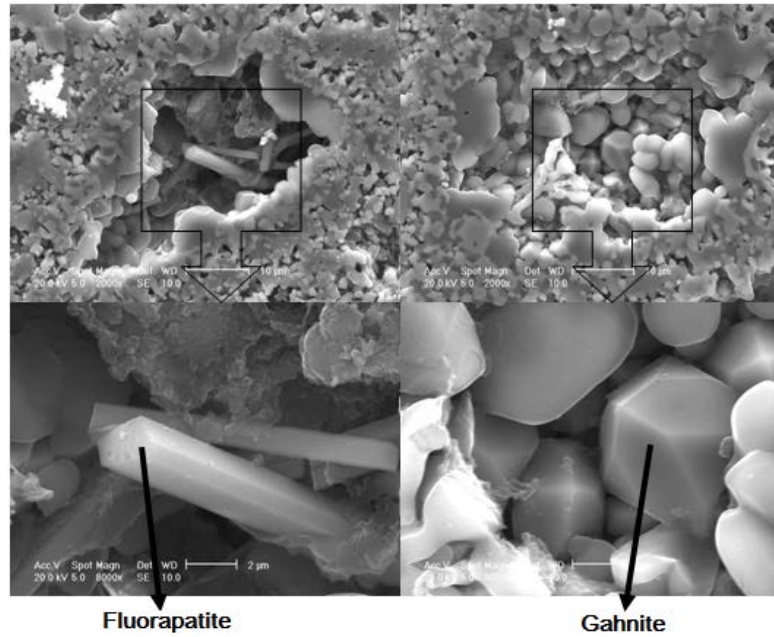


**Figure 11:** SEM and EDX analysis of 60% and 75% Zn glass-ceramics.

#### 4. Discussion

The measured density values were increased linearly with increasing the zinc molar content (Figure 1). The substitution of zinc for calcium resulted in increasing the density of glass as zinc has a larger atomic weight ( $AW=65.3$ ) than the atomic weight ( $AW=40$ ) of calcium, although the atomic radius of Zn (134 pm) [17] is significantly smaller than the atomic radius of calcium (197 pm) [17]. Since the atomic weight of zinc and calcium are significantly different, the linear increase of density indicates that the atomic weight change has a more important effect on the density values than the atomic radius. Consequently, it was observed that zinc substitution can lead to both an increase in glass and oxygen density. In the glass network, the oxygen density reflects the degree of packing of atoms. There is a slight linear increase in the oxygen density from 0% Zn to 60% Zn glasses, indicating a closer packed glass network. It has

been reported [5], that in a similar glass composition with 25, 50, 75 and 100% barium substitution for calcium ( $4.5\text{SiO}_2\text{-}3\text{Al}_2\text{O}_3\text{-}1.5\text{P}_2\text{O}_5\text{-}3\text{BaO-}2\text{BaF}_2$ ), the oxygen density of glasses showed a linear decrease suggesting that barium substitution for calcium resulted in an expanded glass network. It is worth noticing, that barium has an atomic radius of 215 pm larger than the atomic radius of calcium (197 pm) [17]. Similarly, the measured density values for the glass ceramics were increased with increasing the molar content of zinc (Figure 3). This was due to the density dependent on the type of phases as well as the amount of each phase formed in the glass ceramics. For example, the density of crystal phases such as Ca-FAP [ $\text{Ca}_5(\text{PO}_4)_3\text{F}$ ], Mullite ( $\text{Al}_6\text{Si}_2\text{O}_{13}$ ), Gahnite ( $\text{ZnAl}_2\text{O}_4$ ), Calcium Zinc Phosphate [ $\text{CaZn}_2(\text{PO}_4)_2$ ] and Cristobalite ( $\text{SiO}_2$ ) are 3.15, 3.00, 4.62, 3.9 and  $2.27\text{ g/cm}^3$ , respectively [18]. With increasing zinc substitution, both fluorapatite and mullite were replaced by calcium zinc phosphate and gahnite and as a consequence 75%Zn glass ceramic exhibited the highest density value, while the 0%Zn glass ceramic exhibited the lowest value.

The lowest glass transition temperature was  $616^\circ\text{C}$  for the 60%Zn (and  $595^\circ\text{C}$  for the partly crystallised 75%Zn fine particle size glass), suggesting that with increasing zinc content in the glass, more zinc ions can enter the glass network, affecting the glass microstructure and chemical bonding. The question is whether zinc takes part in the glass network formation. We think that most likely this is not the case and zinc may result to phase separation competing for aluminium with silicon [19]. It has been reported [20-22], that the mixed cation effect can be present in glasses and represents the nonlinear variations of properties related to the cation movement and structural

properties, when one type of cation in glass is gradually replaced by another under unvarying total cation content. Rao et al. [23] reported, that the glass transition temperatures of  $x\text{K}_2\text{O}-(40-x)\text{Na}_2\text{O}-50\text{B}_2\text{O}_3-10\text{As}_2\text{O}_3$  system were negatively deviated from linearity (0  $x \leq 40$ ) following the order  $T_g$ .

likely, that the lower  $T_g$  in our case is due to the above described mixed cation effect.

It is interesting to observe, that there are two crystallisation temperatures in both 0%Zn and 25%Zn glasses. As reported previously for the 0%Zn glass [11], the first crystallisation temperature (around 620°C) was due to the fluorapatite formation, whereas the second crystallization temperature was due to the mullite formation and crystal growth of both mullite and fluorapatite. Similarly, the first crystallisation temperature in the 25%Zn glass corresponded to the fluorapatite phase, whereas the second crystallisation temperature corresponded to fluorapatite crystal growth as well as mullite and gahnite phase formation. As zinc content increased, only one crystallisation temperature was observed and as mentioned in section 3.2, the 60%Zn glass (and partly crystallised 75%Zn glass) crystallised mainly to gahnite and cristobalite as well as to a minor phase of zinc calcium phosphate and fluorapatite. It seems that the high zinc content glasses separated into a zinc aluminium rich phase, a silicon rich phase and a zinc-calcium-phosphorus rich phase. The 100% zinc substituted glass was not possible to form as it crystallised rapidly, suggesting that most likely zinc disrupted the glass network leading to phase separation. The endothermic transition at around 1200°C was thought to be due to crystal dissolution which increased with increasing zinc substitution [24].

Zinc containing glasses of different particle size ( $<45\mu\text{m}$  and  $45\text{-}100\mu\text{m}$ ) were studied by DSC analysis from room temperature to  $1300^{\circ}\text{C}$  at a heating rate of  $10^{\circ}\text{C}/\text{min}$ . Bulk crystallization is generally manifested by the independence of the crystallisation peak temperatures from the particle size, while the opposite suggests dependence from the surface area and therefore surface crystallisation [25]. Previous work suggested that the calcium base glass exhibited mainly bulk crystallisation and the crystallisation temperatures were not dependent on the particle size of glass. However, the 25%Zn glass showed dependency of both crystallisation temperatures on the glass particle size (Figure 4), suggesting surface crystallisation. Similarly, the 60%Zn glass (and partly crystallised 75%Zn glass) showed a similar behaviour. It is clear, that the zinc substituted glass is different than the calcium base glass and therefore it is expected that the crystallisation mechanism and phases formed should be also different [26]. It is worth noticing, that all the thermogravimetric analysis was conducted on fine powder glass samples and it was expected that if there was a weight loss this should be due to the larger surface area. It is suggested and is discussed further later, that there is a small fluorine loss from the surface of the glasses due to possibly  $\text{SiF}_4$  formation during heating.

Figure 8 (b) shows the X-ray powder diffraction pattern of zinc containing glass-ceramics heat treated at  $1100^{\circ}\text{C}$  for 1 hour. It is obvious, that with zinc substitution significant changes in the X-ray diffractograms occurred. It is particularly clear, that the peaks associated with the presence of fluorapatite gradually disappeared with substitution, whereas new peaks appeared. There seems to be a

consistent tendency of the glasses with Zn substitution to form a zinc and aluminium rich phase that may result in aluminium not being available to form silicon and aluminium rich phases (lack of mullite). It has been reported [5] that magnesium substitution for calcium in the same glass composition  $4.5\text{SiO}_2\text{-}3\text{Al}_2\text{O}_3\text{-}1.5\text{P}_2\text{O}_5\text{-}3\text{CaO-}2\text{CaF}_2$  resulted in the formation of wagnerite and mullite. However, in the 60%Zn glass ceramic (and 75%Zn glass ceramic), a minor fluorapatite phase was present, indicating that some of the fluorine was involved in this phase. No other fluorine phase was identified. What did happen to the fluorine present in the glass before the heat treatments? As it is suggested from the results, increasing the zinc content resulted in the formation of a zinc and aluminium rich phase as well as a silicon phase (cristobalite). It is therefore likely, that fluorine not forming fluorapatite would be available to form  $\text{SiF}_4$  that would escape during heat treatments from the surface of the fine glass particles. According to Rabinovich et al., volatilisation of fluorine as  $\text{SiF}_4$  occurs in acid melts, but is significantly reduced with increasing basicity of the melt [27]. It has been suggested, that the presence of aluminium in a similar glass composition would lead to the formation of an alumino-silicate network reducing the possibility for available silicon to form  $\text{SiF}_4$  [28]. Therefore, if an aluminium rich phase was present and the glass was phase separated, it would then be possible for  $\text{SiF}_4$  to form easier. It is suggested consequently, that in the case of high zinc content, glass phase separation may lead to the formation of volatile  $\text{SiF}_4$  and therefore subsequent loss of fluorine ions.

The etched surface of the 0%Zn glass ceramic shown in Figure 9 was very similar to

the etched surfaces observed in previous work where needle-like fluorapatite was present [5]. It is also worth noticing, that the needle-like crystals have a hexagonal profile and directivity typical to fluorapatite crystals [29]. Gahnite on the other hand, appears as a polygonal crystal phase (possibly octagonal) [32] as shown in Figures 10 and 11. The atomic ratio of Zn/Al in the crystal phase is 0.5 as estimated by the EDX analysis and is in good agreement with the Al/Zn ratio in the chemical formula of gahnite.

Gahnite ( $\text{ZnAl}_2\text{O}_4$ ) is widely used as ceramic, electronic and catalytic material. It can be synthesized by using conventional ceramic processing techniques, sol-gel, co-precipitation or alumina impregnating methods following calcinations at relatively high temperatures (800-1000°C). Gahnite is characterized by its prominent performance such as high melting temperature (1950°C), low thermal expansion coefficient ( $5.5 \times 10^{-6}/^\circ\text{C}$ , 25-1000°C) as well as high thermal stability and good resistance to acids and bases [12]. Gahnite ( $\text{ZnAl}_2\text{O}_4$ ) is also a ceramic, which is considered a possible transparent conducting oxide (TCO) due to its wide band gap and transparency in UV [31]. In addition, it has been reported that strontium – hardystonite – gahnite has a significant potential for use in surgical procedures where bone regeneration under load-bearing is required [32]. On the other hand, gahnite in glass-ceramic results in increased fracture toughness and wear resistance [33]. It is therefore, worth mentioning that gahnite brings new characteristics to the glass ceramics under study and opens possibly new avenues for applications to explore in research areas outside the biomedical.

## **5. Conclusions**

The density of zinc substituted glasses and glass-ceramics both increased with increasing zinc content. An increase of oxygen density indicates a closer packed glass network. The glass transition temperature decreased with zinc substitution, whereas the crystallization temperature was affected by the particle size of glasses. The crystallisation temperature of fine glass particles was generally increased with increasing substitution. Above 60% of zinc substitution only one crystallisation temperature was observed. It is suggested, that there is some fluorine loss from the surface of the glasses due to possibly  $\text{SiF}_4$  formation during heating. Fluorapatite and mullite phases are present in the calcium base glass ceramics. Gahnite ( $\text{ZnAl}_2\text{O}_4$ ) and calcium zinc phosphate  $[\text{CaZn}_2(\text{PO}_4)_2]$  were formed with increasing zinc substitution for calcium, whereas crystallisation of both mullite and fluorapatite was not favoured. Fluorapatite appeared as a typical needle-like crystal phase with hexagonal profile whereas gahnite appeared as a polygonal (possibly octagonal) crystal phase. The formation of gahnite during the crystallisation of Zn containing glasses offers high potential for the use of these glasses and glass ceramics in research fields other than the biomedical such as semiconducting materials.

## **Acknowledgments**

The authors would like to thank Prof R. Hill of Queen Mary University of London for providing the 60%Zn substituted glass sample as well as Mr. Paul Stanley for assistance with SEM and Mr. Frank Binddlestone for assistance with the use of DSC and TGA.



## References

- [1] W. Höland, P. Wange, Control of phase formation processes in glass-ceramics for medicine and technology, *J. Non-Cryst. Solids* 129 (1991) 152-162.
- [2] A. Clifford, R. Hill, The influence of calcium to phosphate ratio on the nucleation and crystallization of apatite glass-ceramics, *J. Mater. Sci.-Mater. M.* 12 (2001) 461-469.
- [3] A. Stamboulis, R. G. Hill, Characterization of the structure of calcium alumino-silicate and calcium fluoro-alumino-silicate glasses by magic angle spinning nuclear magnetic resonance (MAS-NMR), *J. Non-Cryst. Solids* 333 (2004) 101-107.
- [4] R. G. Hill, A. Stamboulis, Characterisation of fluorine containing glasses by  $^{19}\text{F}$ ,  $^{27}\text{Al}$ ,  $^{29}\text{Si}$  and  $^{31}\text{P}$  MAS-NMR spectroscopy, *J. Dent.* 34 (2006) 525-532.
- [5] F. Wang, Cation substitution in ionomer glasses: effect on glass structure and crystallization, PhD thesis (2009), University of Birmingham.
- [6] A. Sabareeswaran, B. Basu, Early osseointegration of a strontium containing glass ceramic in a rabbit model, *Biomaterials* 34 (2013) 9278-9286.
- [7] D. Boyd, M. R. Towler, R. V. Law, R. G. Hill, An investigation into the structure and reactivity of calcium-zinc-silicate ionomer glasses using MAS-NMR spectroscopy, *J. Mater. Sci.-Mater. M.* 17 (2006) 397-402.
- [8] B. E. Yekta, P. Alizadeh, L. Rezazadeh, Synthesis of glass-ceramic glazes in the  $\text{ZnO-Al}_2\text{O}_3\text{-SiO}_2\text{-ZrO}_2$  system, *J. Eur. Ceram. Soc.* 27 (2007) 2311-2315.
- [9] G. Lusvardi, G. Malavasi, L. Menabue, and M. C. Menziani, Synthesis,

characterization, and molecular dynamics simulation of Na<sub>2</sub>O-CaO-SiO<sub>2</sub>-ZnO glasses, *J. Phys. Chem. B* 106 (2002) 9753-9760.

- [10] Y.-H. Cho, S.-J. Lee, J. Y. Lee, S. W. Kim, C. B. Lee, W. Y. Lee, and M. S. Yoon, Antibacterial effect of intraprostatic zinc injection in a rat model of chronic bacterial prostatitis, *Int. J. Antimicro. Ag.* 19 (2002) 576-582.
- [11] S. G. Griffin and R. G. Hill, Influence of glass composition on the properties of glass polyalkenoate cements. Part II: influence of phosphate content, *Biomaterials* 21 (2000) 399–403.
- [12] C. M. Gorman and R. G. Hill, Heat-pressed ionomer glass-ceramics. Part II. Mechanical property evaluation, *Dent. Mater.* 20 (2004) 252-261.
- [13] C. Wu, J. Chang, W. Zhai, A novel hardystonite bioceramic: preparation and characteristics, *Ceram. Int.* 31 (2005) 27–31.
- [14] X. Cheng Li, Study on synthesis and preparation of corundum/mullite /gahnite-based multiphase materials, Master's thesis (2003), Wuhan University of Science and Technology.
- [15] V. Aina, A. Perardi, L. Bergandi, G. Malavasi, L. Menabue, C. Morterra, D. Ghigo, Cytotoxicity of zinc-containing bioactive glasses in contact with human osteoblasts, *Chem.-Biol. Inter.* 167 (2007) 207-218.
- [16] S. Kapoor, A. Goel, A. Tilocca, V. Dhuna, G. Bhatia, K. Dhuna, J.M.F. Ferreira, Role of glass structure in defining the chemical dissolution behavior, bioactivity and antioxidant properties of zinc and strontium co-doped alkali-free phosphosilicate glasses, *Acta Biomater.* 10 (2014) 3264-3278.

- [17] J. C. Slater, Atomic radii in crystals, *J. Chem. Phys.* 41 (1964) 3199–3205.
- [18] S. W. Kieffer, Thermodynamics and lattice vibrations of minerals: 1. Mineral heat capacities and their relationships to simple lattice vibrational models, *Rev. Geophys. Space Physics* 17 (1979) 1-19.
- [19] B. K. Chethana, C. N. Reddy, Thermo-physical and structural studies of sodium zinc borovanadate glasses in the region of high concentration of modifier oxides, *Mater. Res. Bull.* 47 (2012) 1810-1820.
- [20] A. G. Hunt, Mixed-alkali effect: some new results, *J. Non-Cryst. Solids* 255 (1999) 47-55.
- [21] J. M. Bobe, J. M. Reau, J. Senegas, and M. Poulain, Ion conductivity and diffusion in  $\text{ZrF}_4$ -based fluoride glasses containing  $\text{LiF}$  ( $0 \leq x_{\text{LiF}} \leq 0.60$ ), *J. Non-Cryst. Solids* 209 (1997) 122-136.
- [22] A. Pradel and M. Ribes, Ion transport in superionic conducting glasses, *J. Non-Cryst. Solids* 172-174 (1994) 1315- 1323.
- [23] N. Srinivasa Rao, S. Bale, M. Purnima, K. Siva Kumar, and S. Rahman, Mixed alkali effect in boroarsenate glasses, *J. Phys. Chem. Solids* 6 (2007) 1354-1358.
- [24] M. D. O'Donnell, N. Karpukhina, Real time neutron diffraction and solid state NMR of high strength apatite–mullite glass ceramic, *J. Non-Cryst. Solids* 356 (2010) 2693-2698.
- [25] Y. Takahashi, Y. Yamazaki, Perfect surface crystallization and parasitic structures in nonstoichiometric glass-ceramics: Micro-/nanoscopic aspects, *Appl. Phys. Lett.* 102 191903 (2013); doi: 10.1063/1.4805028.

- [26] H. Zreiqat, Y. Ramaswamy, The incorporation of strontium and zinc into a calcium–silicon ceramic for bone tissue engineering, *Biomaterials* 31 (2010) 3175-3184.
- [27] E. M. Rabinovich, On the structural role of fluorine in silicate glasses, *Phys. Chem. Glasses* 24 (1983) 54–56.
- [28] R. Hill, D. Wood, and M. Thomas, Trimethylsilylation analysis of the silicate structure of fluoro-alumino-silicate glasses and the structural role of fluorine, *J. Mater. Sci.* 34 (1999) 1767-1774.
- [29] M. D. O'Donnell and R. G. Hill, Neutron diffraction of chlorine substituted fluorapatite, *Mater. Lett.* 63 (2009) 1347-1349.
- [30] E. Tkalec and S. Kurajica, Crystallization behaviour and microstructure of powdered and bulk ZnO–Al<sub>2</sub>O<sub>3</sub>–SiO<sub>2</sub> glass-ceramics, *J. Non-Cryst. Solids* 351 (2005) 149-157.
- [31] H. Dixit and N. Tandon, First-principles study of possible shallow donors in ZnAl<sub>2</sub>O<sub>4</sub> spinel, *Phys. Rev. B* 87 (2013) 174101.
- [32] S. I. Roohani-Esfahani and C. R. Dunstan, Unique microstructural design of ceramic scaffolds for bone regeneration under load, *Acta Biomater.* 9 (2013) 7014-7024.
- [33] D. Herman and T. Okupski, Wear resistance glass-ceramics with a gahnite phase obtained in CaO-MgO-ZnO-Al<sub>2</sub>O<sub>3</sub>-B<sub>2</sub>O<sub>3</sub>-SiO<sub>2</sub> system, *J. Eur. Ceram. Soc.* 31 (2011) 485-492.